Synthesis and investigation of imidazolium functionalized poly(arylene ether sulfone)s as anion exchange membranes for all-vanadium redox flow batteries

Di Lu,[a] Lele Wen,*[ab] Feng Nie[a] and Lixin Xue*[a]

A serials of imidazolium functionalized poly(arylene ether sulfone) as anion exchange membranes (AEMs) for all-vanadium redox flow battery (VRB) application are synthesized successfully in this study. The AEMs obtained with different ionization levels, Im-PAES-0.5/0.7/1.1 (0.5/0.7/1.1 represents the different degrees of bromination, respectively) membranes are intensively characterized. Compared with commercial Nafion 117 membrane, the vanadium ion permeation values of AEMs are lower while their chemical stability in VO^{2+} are comparable. The ionic conductivities, vanadium ion permeability, stability of the membranes and their performance in VRB cells are greatly affected by ionic exchange capacity (IEC). In order to balance these important performance factors, the Im-PAES-0.7 membrane with a moderate IEC of 2.01 meq g^{-1} exhibits good stability, high ionic conductivity and low vanadium ion permeation, resulting in high voltage efficiencies (up to 87.5%), high coulombic efficiencies (up to 96.1%), as well as high energy efficiency. The VRB cell with the Im-PAES-0.7 membrane achieves comparable to or even slightly higher energy efficiency values (up to 81.7%) than those of Nafion 117 membranes (up to 78.9%) in the current density range of 60–120 mA cm^{-2}. During 40 charge–discharge cycles at different current densities, the Im-PAES-0.7 anion exchange membrane exhibits a comparable short-term stability to Nafion 117 membrane.

1. Introduction

All-vanadium redox flow batteries (VRBs) have received more and more attention during the past decades for their deep-discharge capability, flexible design, long cycle life, fast response time and low cost.[1–3] They are being considered as a promising energy storage system for electric vehicles and large-scale grid connected equipment.[4–6] As a core component of the VRB system, the ion exchange membrane (IEM) not only separates two side of electrolytes to prevent cross-contamination, but also provides ionic conduction channels to balance the charge of electrolytes and complete the circuit during the charge–discharge cycle process.[7,8]

An ideal IEM for the VRB application should have high ionic conductivity, low permeability of vanadium ions, good chemical stability, mechanical property and low cost.[9,10] Currently, Nafion membranes are used as common IEMs for commercial VRB cells since their high ionic conductivities, excellent chemical and mechanical properties.[7] However, till now, their applications are still limited by intrinsic high permeability of vanadium ions and high cost.

To seek improved alternative IEMs for the VRB, efforts have been devoted to modifying Nafion membranes[11–13] and developing membranes with novel chemical structures.[14–20] Anion exchange membranes (AEMs), having higher barrier property for the positively charged vanadium ions from the Donnan exclusion effect, have been reported with improved performance in VRB.[21–29] However, conventional ammonium based cationic structures on the AEMs tend to have low chemical stability in the VRB environment.

Owing to the existence of the conjugated π bond in the unique N-heterocyclic structure, imidazolium based structures exhibit not only high ionic conductivity, but also high oxidation resistance, good chemical and thermal stability. In the past several years, imidazolium-containing polymers have been greatly developed and used as anion exchange membranes for alkaline fuel cells (AFCs).[30–38] However, the imidazolium contained AEMs for VRB cells application are rarely reported. Recently, Fang and co-workers synthesized a novel type of anion exchange membrane based on poly(2,2,2-trifluoroethyl methacrylate-*co*-*N*-vinyl imidazole) for the VRB application. It was

[a]*Polymer and Composite Division, Key Laboratory of Marine Materials and Related Technologies, Zhejiang Key Laboratory of Marine Materials and Protective Technologies, Ningbo Institute of Material Technology & Engineering, Chinese Academy of Sciences, Ningbo, Zhejiang, 315201, China. E-mail: wenlele@nimte.ac.cn; xuelx@nimte.ac.cn*

[b]*Key Laboratory of Organofluorine Chemistry, Shanghai Institute of Organic Chemistry, Chinese Academy of Sciences, Shanghai, 200032, China*

found that this type of AEM exhibited significantly low permeability of vanadium ions and good chemical stability in electrolytes.[39]

To further explore more kinds of imidazolium-containing AEMs and investigate the relationship of "structure–property" of AEMs for applications in VRB. Herein, we reported on a serials of imidazolium functionalized poly(arylene ether sulfone) AEMs for the application of VRB cells. The readily available raw materials, including methylhydroquinone (M-HQ) and/or 2,3,5-trimethylhydroquinone (TM-HQ) with 4,4′-dichlorophenylsulfone (DCPS), are employed to construct the polymer backbone. The properties of the obtained membranes, including ionic conductivity, ion exchange capacity (IEC), water uptake, chemical stability, vanadium permeability as well as cell charge–discharge cycling performance were carefully investigated.

2. Experimental

2.1 Materials

Methylhydroquinone (M-HQ), potassium carbonate (K_2CO_3), 4,4′-dichlorophenylsulfone (DCPS), 2,3,5-trimethylhydroquinone (TM-HQ), *N*-bromosuccinimide (NBS), 1,1,2,2-tetrachloroethane (TTCE), benzoyl peroxide (BPO), *N*-methylimidazole and magnesium sulfate ($MgSO_4$) were all purchased from Aladdin Industrial Inc.; vanadium oxysulfate ($VOSO_4$, 98%) was purchased from Shanghai Luyuan Fine Chemical Plant. All other chemicals were supplied from Shanghai Sinopharm Chemical Reagent Co., Ltd. (China) and used without further purification.

2.2 Preparation of anion exchange membrane

The preparation processes of imidazolium functionalized poly(arylene ether sulfone) polymers were illustrated in Schemes 1 and 2, respectively.

2.2.1 Synthesis of M-PAES. M-PAES (shown in Scheme 1) was synthesized *via* a general polycondensation reaction. Methylhydroquinone (24 g, 0.193 mol), 4,4′-dichlorophenylsulfone (55.5 g, 0.193 mol), potassium carbonate (32.4 g, 0.234 mol), toluene (55 ml) and tetramethylene sulfone (TMS, 90 ml) were placed into a 500 ml three-necked round-bottomed flask equipped with a Dean–Stark trap, a condenser, a mechanical stirrer, and a gas inlet and outlet. The mixture was heated at 150 °C for 3 h to completely get rid of water in the mixture. After toluene in the mixture was completely removed, additional 150 ml of tetramethylene sulfone was added and the reaction mixture was heated at 200 °C for 5 h. The reaction mixture was poured into large excess deionized water under vigorous stirring after the temperature was below 150 °C. The formed resin was subsequently washed by deionized water with several times and dried under vacuum at 80 °C for 48 h to obtain the desired homopolymer which was named as M-PAES (M_n: 53 K, M_w: 118 K).

The synthetic route for another 2,3,5-trimethylhydroquinone based copolymer which was named as TM-PAES (shown in Scheme 2) (M_n: 47 K, M_w: 104 K) was similar as M-PAES.

2.2.2 Bromination. The preparation procedure of BM-PAES was set as a typical example for bromination reaction: M-PAES (5 g) and 1,1,2,2-tetrachloroethane (TTCE, 100 ml) were added to a 250 ml three-necked round-bottomed flask equipped with a condenser, a magnetic stirrer. When the M-PAES polymer was completely dissolved, *N*-bromosuccinimide (NBS, 2.3 g, 13 mmol) and benzoyl peroxide (BPO, 0.16 g, 0.65 mmol) were added subsequently into the reaction mixture. The solution was heated at 85 °C for 5 h under nitrogen atmosphere. Afterwards, the mixture was cooled to room temperature, and poured into 250 ml of ethanol. The formed fibrous polymer was washed by ethanol with several times continuously and dried under vacuum at 60 °C for 24 h to obtain the desired BM-PAES polymer, which BM denotes the brominated product.

2.2.3 Preparation of Im-PAES membranes. The typical procedure for the preparation of Im-PAES membrane: BM-PAES (1 g) was dissolved in *N*-methy-2-pyrrolidone (NMP) to form a 10 wt% solution, and followed addition of *N*-methylimidazole (492 mg, 6.0 mmol) at 50 °C. After 24 h, the reaction mixture was casted onto a clean and smooth glass plate, and the glass plate was completely dried under atmosphere at 70 °C for 24 h. In order to remove the residual *N*-methylimidazole within the membrane, the as-prepared membrane was immersed into a 5 wt% HCl aqueous for 24 h, as a result, the desired chloride (Cl^-) form Im-PAES membrane was obtained after washing with deionized water.

2.3 Polymer and membrane characterization

2.3.1 ^{1}H NMR and FT-IR spectroscopy. Using 400 MHz spectrometer (Bruker) to record ^{1}H NMR spectra. Deuterated dimethyl sulfoxide (DMSO-d_6) was used as the solvent. FT-IR spectra of the samples were analyzed in the range of 3500–950 cm^{-1} by using a Thermo-Niclolet 6700 spectrometer.

2.3.2 GPC measurement. The molecular weight (M_n) and molecular weight distribution (M_w/M_n) of the polymers were measured by using a gel permeation chromatography (PL-GPC 220) equipped with Agilent 1260 Infinity pump, a refractive index (RI) detector. Chloroform ($CHCl_3$) was used as the eluent with a flow rate of 1.0 ml min^{-1} at 40 °C. Molecular weight was calibrated with standard polystyrene samples.

2.3.3 Water uptake (WU). The water uptake of the Im-PAES membrane (in chloride form) was measured by immersing the membrane sample in deionized water at 25 °C for 24 h. Then, the membrane was taken out, the excess water on the surface was wiped out by using absorbent paper and weighed immediately. Afterwards, the membrane was dried under vacuum at 60 °C for at least 48 h, and the membrane was weighed again until the weight was invariable. The water uptake was calculated according to the following equation:

$$\mathrm{WU}(\%) = \frac{(W_{\mathrm{wet}} - W_{\mathrm{dry}})}{W_{\mathrm{dry}}} \times 100\% \quad (1)$$

where W_{wet} and W_{dry} are the mass of the membrane in the wet and dry states, respectively.

2.3.4 Swelling ratio (SR). The linear swelling ratio was measured to evaluate the dimensional stability of the anion

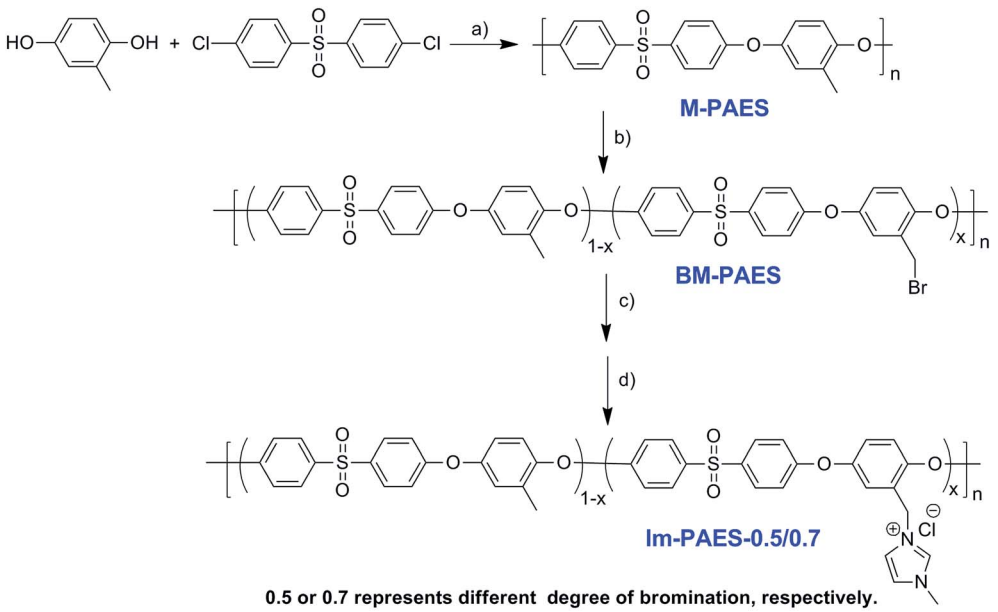

Reaction condition: a) K_2CO_3, Toluene, TMS, 150 °C for 3h, 200 °C for 5 h; b) NBS, BPO, $C_2H_2Cl_4$, 85 °C; c) 1-methylimidazolium, N-methyl-2-pyrrolidone, 50 °C; d) Cast film.

Scheme 1 Synthetic route of Im-PAES-0.5/0.7 anion exchange membranes.

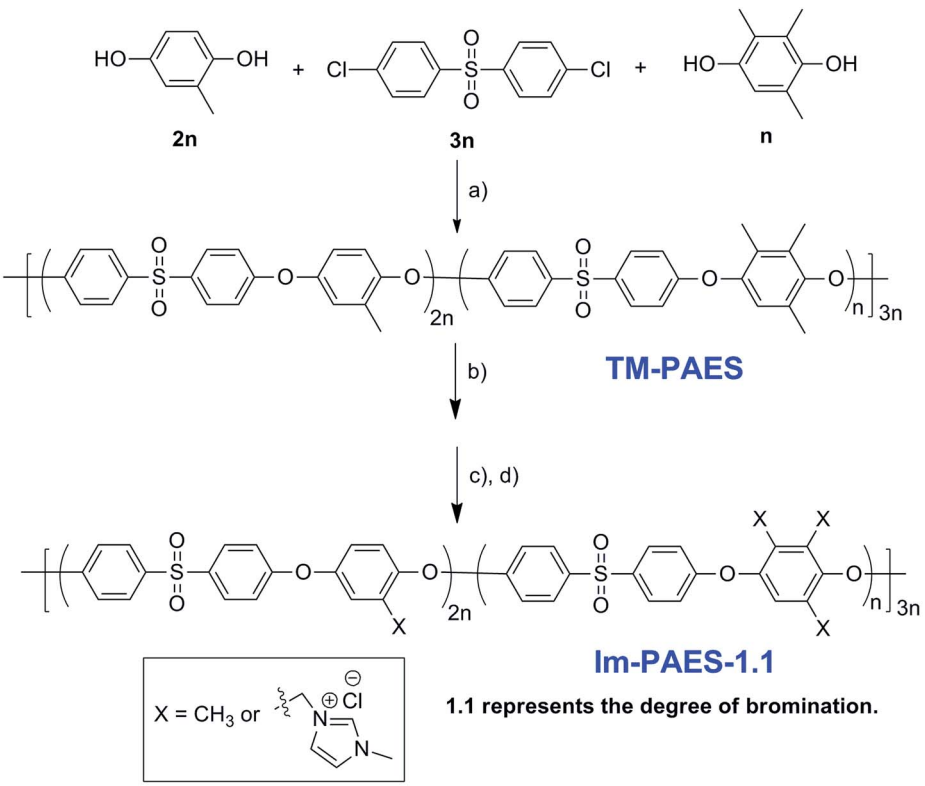

Reaction condition: a) K_2CO_3, Toluene, TMS, 150 °C for 3h, 200 °C for 5 h; b) NBS, BPO, $C_2H_2Cl_4$, 85 °C; c) 1-methylimidazolium, N-methyl-2-pyrrolidone, 50 °C; d) Cast film.

Scheme 2 Synthetic route of Im-PAES-1.1 anion exchange membranes.

membrane. Firstly, the membrane sample was dried under vacuum at 60 °C for 48 h, and the lengths of membrane was measured. Afterwards, the membrane was soaked in deionized water for 24 h and the length of the membrane was measured again. The swelling ratio was calculated using the following equation:

$$\mathrm{SR}(\%) = \frac{L_1 - L_0}{L_0} \times 100\% \quad (2)$$

where L_1 and L_0 are the lengths of the wet membrane and dry membrane, respectively.

2.3.5 Ion exchange capacity (IEC). The ion exchange capacity (IEC) was determined by titration method. The Im-PAES membrane was accurately weighed and immersed in 25 ml of 0.1 M $NaNO_3$ solution for 48 h at room temperature to undergo complete ionic exchange process. Afterwards, the solution was titrated with 0.1 M $AgNO_3$ standard solution and K_2CrO_4 (5 wt%) was used as the indicator. IEC (meq g^{-1}) was calculated using the following equation:

$$\mathrm{IEC} = \frac{V_{\mathrm{AgNO_3}} \times C_{\mathrm{AgNO_3}}}{M_{\mathrm{dry}}} \quad (3)$$

where $V_{\mathrm{AgNO_3}}$ is the volume of consumed $AgNO_3$ standard solution, $C_{\mathrm{AgNO_3}}$ is the concentration of $AgNO_3$ standard solution, and M_{dry} is the weight of dry membrane, respectively.

2.3.6 Ionic conductivity. The ionic conductivity of the membrane sample was determined *via* AC impedance spectroscopy with a Zehner electrochemical equipment (Germany) in the frequency ranging from 0.1 Hz to 100 kHz. The area resistance (R) of Im-PAES anion exchange membrane was measured at Zehner electrochemistry working station by the two-probe method in deionized water. The ionic conductivity σ (S cm^{-1}) of the membrane sample was calculated using the following formula:

$$\sigma = \frac{l}{RA} \quad (4)$$

where l is the distance between the two electrodes (cm), A is the area of cross section (cm^2), R is the membrane resistance (Ω).

2.3.7 Permeability of VO^{2+}. The permeability of VO^{2+} ions across the membrane was measured *via* the following method. The membrane was pressed between two half-cells with graphite felts on both sides to prevent the leakage of electrolyte. One side was filled with the solution of 1.5 M $VOSO_4$ in 3 M H_2SO_4, and the other side was filled with the solution of 1.5 M $MgSO_4$ in 3 M H_2SO_4. Herein, $MgSO_4$ was used to equalize the ionic strength of the two sides and minimize the osmotic pressure effects. The volume for each side was same 45 ml and the membrane area exposed in the solution was 9 cm^2. 1 ml of $MgSO_4$ solution sample was taken out at intervals to test the VO^{2+} ions permeability by using a UV-Visible spectrophotometer. The permeability of vanadium ions through the membranes can be calculated using the following equation:

$$V\frac{\mathrm{d}C_t}{\mathrm{d}t} = S\frac{P}{L}(C_0 - C_t) \quad (5)$$

where V is the volume of the solution in both sides, S is the area of the membrane exposed in the solution, P is the permeability parameter of vanadium ions, L is the thickness of the membrane samples, C_0 is the initial concentration of the vanadium ions and C_t is the vanadium ions concentration in $MgSO_4$ solution at time t, respectively.

2.3.8 Chemical stability. The chemical stability of Im-PAES membranes was evaluated and measured through the weight loss of membrane in 1.5 M VO_2^+ solution within 10 days. The dry membrane was firstly immersed into deionized water for 24 h, and then the wet membrane sample was weighted after the water on the surface of membrane was completely wiped out. Immersing the membrane sample into the solution of 1.5 M VO_2^+ (V) in 3 M H_2SO_4, and then the accurate weight of the membrane sample was obtained every day.

2.4 Cell cycling performance

The cell charge–discharge cycling test was carried out according to the method depicted in the literature.[26] Initially, the membrane (6 cm^2) was sandwiched between two pieces of carbon felts, and the thickness and area of carbon felts were 5 mm and 6 cm^2, respectively. Two pieces of graphite plates were employed as current collectors (thickness: 4 mm). The negative electrolyte was the solution of 1.5 M V^{3+} in 3 M H_2SO_4 and the positive electrolyte was the solution of 1.5 M V^{4+} in 3 M H_2SO_4. Injecting 30 ml of the negative and the positive electrolytes in two tanks, respectively. The flowing rate of the electrolytes was 30 ml min^{-1}. The charge–discharge cycling was performed at current density of 60, 80, 120 mA cm^{-2}, respectively. The upper limit voltage was charged to 1.7 V and the lower voltage limit was 0.8 V. The cell efficiencies of the cell were calculated using the following equations:

$$\mathrm{CE} = \frac{C_\mathrm{d}}{C_\mathrm{c}} \times 100\% \quad (6)$$

$$\mathrm{EE} = \frac{E_\mathrm{d}}{E_\mathrm{c}} \times 100\% \quad (7)$$

$$\mathrm{VE} = \frac{\mathrm{EE}}{\mathrm{CE}} \times 100\% \quad (8)$$

where C_d is the discharge capacity and C_c is the charge capacity of the cell, E_d is the discharge energy and E_c is the charge energy of the cell, respectively.

3. Results and discussion

3.1 GPC, ^{1}H NMR and FT-IR spectra

The molecular weight and polydispersity index ($M_\mathrm{w}/M_\mathrm{n}$) of M-PAES and TM-PAES were analyzed with GPC using chloroform eluent, and the results were summarized in Table 1. Both M-PAES and TM-PAES resins exhibited sufficient high molecular weight (M_n > 47 K, as confirmed by GPC) for further membrane formation.

^{1}H NMR spectra of M-PAES, BM-PAES and Im-PAES samples were shown in Fig. 1.

Table 1 Molecular weight and polydispersity index of M-PAES and TM-PAES[a]

Polymer	M_n	M_w	M_w/M_n
M-PAES	53 K	118 K	2.23
TM-PAES	47 K	104 K	2.21

[a] Determined by GPC.

From Fig. 1, it can be seen that the single peak at 2.0 ppm was assigned to the protons of methyl group (H_a). The signal of protons sited at *ortho*-position of phenylsulfonyl was observed at 8.0 ppm (H_f). By comparison of the integral ratio of the protons of H_a and H_f, the structure of M-PAES polymer can be confirmed. After the bromination reaction of the benzyl group, an obvious signal showed at 4.5 ppm which was ascribed to the protons of bromomethyl group (H_b). Afterwards, the signal of H_b was disappeared and a single peak at 5.3 ppm was observed (H_e), indicating that the bromo atom was completely substituted by the *N*-methyl-imidazole ring. Furthermore, the broad peak at 9.2 ppm was attributed to the proton of imidazolium (H_d), as well as the single peak at 3.7 ppm was the typical signal of methyl group attached on the imidazolium structure (H_c). All these results totally confirmed the successful introduction of the imidazolium ring. The degree of functionalization (DF) of Im-PAES polymers was defined as the average number of imidazolium groups on per repeating unit, and could be calculated *via* comparing the ratio of integration value of the above mentioned typical protons.

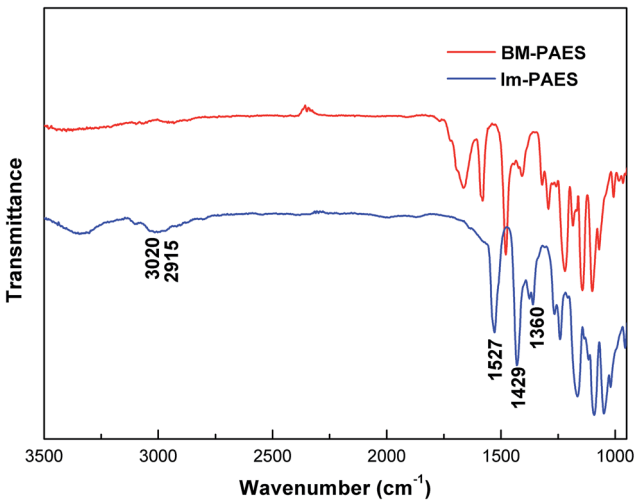

Fig. 2 FT-IR spectra of BM-PAES and Im-PAES samples.

The FT-IR spectra of BM-PAES and Im-PAES samples were shown in Fig. 2. The peak at 3020 cm^{-1} was ascribed to the vibration of aromatic C–H bond. The weak signal at 2915 cm^{-1} was assigned to the vibration of the aliphatic C–H bond on the methyl or methylene groups. The strong signals of the asymmetric and symmetric vibrations of C=C bond on phenyl rings were observed at 1527 and 1429 cm^{-1}, respectively. The peak at 1360 cm^{-1} was mainly attributed to the vibration of C–N bond on the imidazolium group.[40] Both ^{1}H NMR and FT-IR results

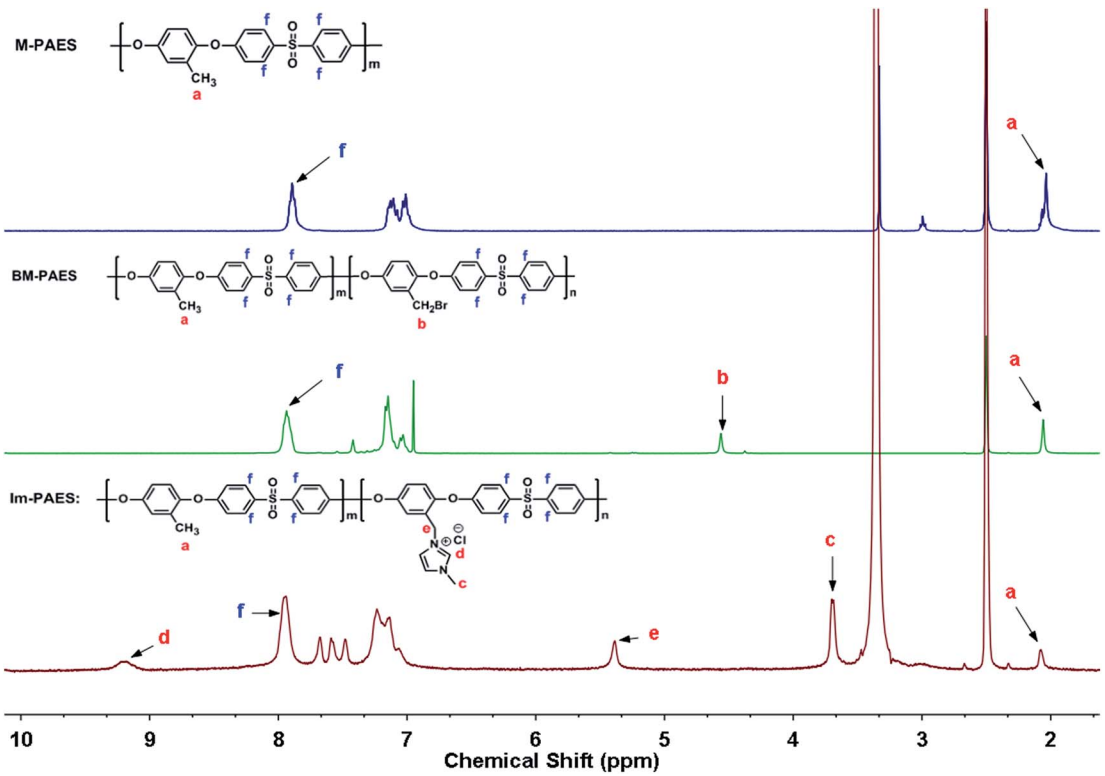

Fig. 1 ^{1}H NMR spectra of M-PAES, BM-PAES and Im-PAES samples.

Table 2 The thickness, water uptake, swelling ratio and ion exchange capacity of the membranes

Membranes	DF[a]	Thickness (μm)	WU[b] (%)	SR[c] (%)	IEC_C[d] (meq g^{-1})	IEC_M[e] (meq g^{-1})
Im-PAES-0.5	0.5	80	7.2	3.3	1.52	1.50
Im-PAES-0.7	0.7	90	23.0	7.1	2.02	2.01
Im-PAES-1.1	1.1	100	37.6	25.9	3.50	3.49

[a] Degree of functionalization (DF) of polymer was determined by ^{1}H NMR. [b] WU represents the water uptake. [c] SR represents the swelling ratio. [d] IEC_C represents the IEC value calculated from ^{1}H NMR. [e] IEC_M represents the measured IEC value by titration.

offered a sufficient evidence to validate the successful synthesis of Im-PAES serials membranes.

3.2 Water uptake (WU), swelling ratio (SR) and ion exchange capacity (IEC)

The water uptake, swelling ratio as well as ion exchange capacity of the prepared anion exchange membranes were summarized in Table 2. It can be seen that the water uptake and swelling ratio of the membranes increased significantly with increasing the content of ion exchange groups, which was mainly attributed to more ion exchange groups can cause higher hydrophilicity and water content of the membrane. As well known, the transport channels for anions could be formed from water clusters inside the membrane. Therefore, the ionic conductivity was closely correlated with the content of ion exchange groups, the higher density of salt groups will promote more efficient movement of anions inside the membrane and higher ionic conductivity would be obtained. Additionally, it was also observed that the measured IEC value was in good accordance with the value calculated from ^{1}H NMR, this result further confirmed that the complete introduction of *N*-methyl-imidazolium.

3.3 Ionic conductivity

Ionic conductivity is a very important parameter to evaluate the membranes for applications in VRB. As shown in Fig. 3, the ionic conductivities of the Im-PAES-0.5 membrane increased from 6.58 to 36.76 mS cm^{-1}, while temperature was changing from 30 to 95 °C. For the Im-PAES-0.7 membrane, a maximum ionic conductivity could be achieved as 73.1 mS cm^{-1} when the temperature increased to 95 °C. Both of the ionic conductivities of Im-PAES membranes kept an significant rising trend as the temperature increasing. This was mainly because of the mobility of anions and the free volume inside the membrane increased with the temperature increasing, which could be beneficial to ionic transmission.[41] Moreover, it was observed that the Im-PAES-1.1 membrane was degraded and dispersed to several pieces when the temperature increased above 60 °C, which was caused by its over-high IEC value. In general, the high ionic conductivity of membrane was gained at the expense of the other aspects of performance, especially mechanical strength and swelling degree.

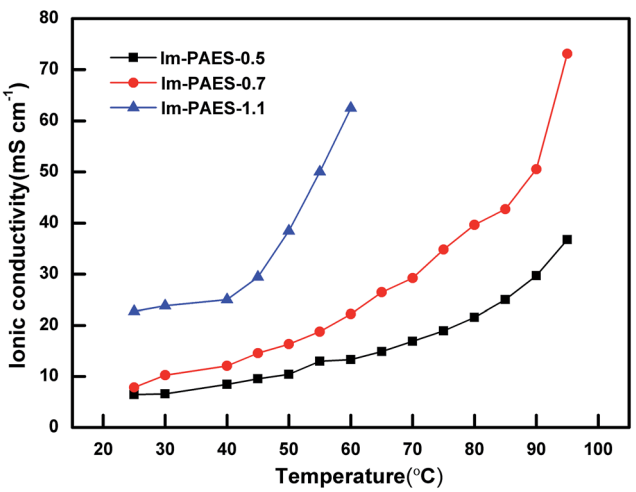

Fig. 3 Temperature dependence of ionic conductivities of Im-PAES-0.5/0.7/1.1 membranes under fully hydrated.

3.4 Solubility

To evaluate the solvent resistance of different kinds of polymers, some polar proton/non-proton solvents were screened and the results were shown in Table 3. It can be seen that except alcohol, acetone and acetonitrile, the brominated resins, BM-PAES exhibited moderate to good solubility in the most of solvents such as *N*-methyl pyrrolidone (NMP), dimethylacetamide (DMAc), dimethylsulfoxide (DMSO) as well as chloroform ($CHCl_3$). Moreover, an obvious comparison can be observed that the solubility of the Im-PAES membranes were poorer than that of BM-PAES, and the solubility decreased with the IEC increasing. This result provided us a design guidance for the AEMs structure with good solvent and acid resistance.

3.5 Permeability of vanadium ions

The permeability of vanadium ions across membrane was a significant factor which can influence the VRB performance,

Table 3 Solubility behavior of the BM-PAES and Im-PAES samples[a]

Membranes	NMP	Acetone	EtOH	DMAc	CH_3CN	DMSO	$CHCl_3$
BM-PAES-0.5	+	−	−	+	−	+	+
BM-PAES-1.1	+	−	−	+	−	+	+
Im-PAES-0.5	+	−	−	+	−	+	±
Im-PAES-0.7	±	−	−	±	−	±	−
Im-PAES-1.1	−	−	−	−	−	−	−

[a] The test was carried out at 25 °C; +, ± and − represent completely soluble, partially soluble and insoluble in the solvent, respectively.

this was mainly because the crossover of vanadium ions through the membrane would cause serious self-discharge of VRB cell system and lead to low coulombic efficiency. According to the eqn (5), the permeability (P) of V(IV) ions was calculated and shown as Fig. 4. Compared with Im-PAES-1.1 and Nafion 117 membranes, the Im-PAES-0.5/0.7 membranes showed quite low vanadium permeability after one day, only about 0.05×10^{-7} cm^2 min^{-1} and 0.07×10^{-7} cm^2 min^{-1}, respectively. Moreover, there was no obvious changes after 10 days for both membranes. These results could be explained by the coulomb repulsion between the cation groups existed inside the membrane and vanadium ions. However, the Im-PAES-1.1 membrane showed much higher vanadium permeability than that of the Im-PAES-0.5/0.7 membranes. We speculated that this abnormal result was mostly attributed to the high water uptake of the Im-PAES-1.1 membrane, which led to the absorption of much vanadium ions from the concentrated side and transmitting to the other blank solution.

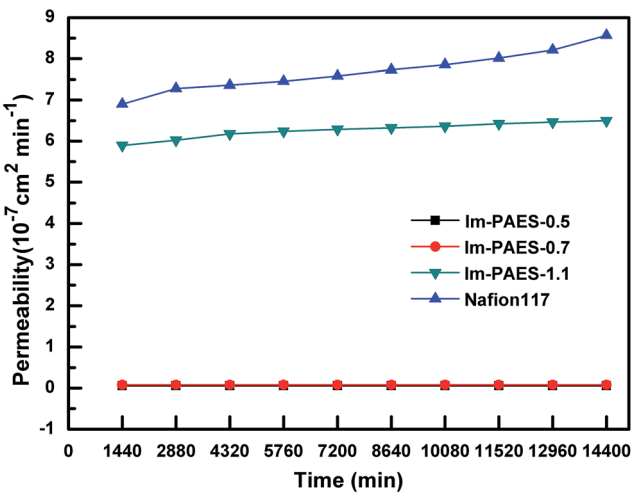

Fig. 4 The permeability of V(IV) ions of Im-PAES and Nafion 117 membranes within 10 days.

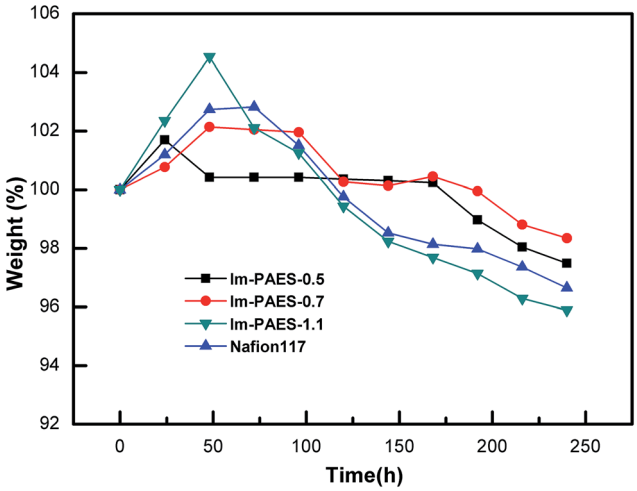

Fig. 5 The weight changes of Im-PAES and Nafion 117 membranes in the solution of 1.5 M VO_2^+ in 3 M H_2SO_4.

3.6 Membrane stability

The chemical stability of the membrane directly influences the VRB cell lifespan. In this work, the stability of Im-PAES membranes in the solution which contained oxidative V(V) ions was also studied. The samples were measured by soaking in a solution of 1.5 M VO_2^+ in 3 M H_2SO_4 at 25 °C for 10 days, and the weight changes of membranes were calculated every day. As shown in Fig. 5, both Im-PAES-0.5 and Im-PAES-0.7 membranes showed slight weight loss of about 3% and 2% during the whole measuring process, respectively. This evidence indicated that the Im-PAES-0.5/0.7 membranes possess at least moderate durability in the strong oxidative VO_2^+ electrolyte. As a result, we believed that the compact structure of two membranes was a beneficial factor to elevate their chemical stability. In contrast, the Im-PAES-1.1 membrane's weight firstly increased up to 3.6% after two days, which was mainly due to the absorption of vanadium ions by the membrane with high water uptake. However, with time increasing, the dramatic weight loss of the membrane reached almost 4.2% on the last day, this result indicated that the Im-PAES-1.1 membrane were less stable. As a comparison, the weight changes of Nafion 117 membrane showed a similar trend with Im-PAES-1.1, owing to the unique structure of Nafion 117, the weight loss was 3.2% in 10 days. In these screening experiments, all these membranes showed comparable short-term stability performance to Nafion membranes. Long term stability of these membranes is being further assessed.

3.7 VRB cell performance

The charge–discharge cycling performance of the VRB cells assembled with Nafion 117 and different Im-PAES membranes were investigated. The coulombic efficiency (CE), voltage efficiency (VE), energy efficiency (EE) as well as cycling stability were shown in Fig. 6–8, respectively.

From Fig. 6, we can see that the CE of VRB cell assembled with Im-PAES-0.7 membrane was slightly higher than that of VRB cell with Nafion 117 membrane at the current densities ranging from 60 to 120 mA cm^{-2}. The CE curves exhibited an unilateral rising trend with increasing current density, and the highest CE was obtained as 96.1% when the current density was 120 mA cm^{-2}. This was mainly attributed to the excellent resistance property of Im-PAES-0.7 to vanadium ions. In addition, higher current density could shorten the charge–discharge time and further reduce the self-discharge of VRB cell. As a typical comparison, the Im-PAES-1.1 membrane, with high permeability of vanadium ions, possessed much lower CE value than that of Nafion 117 membrane. Among all the Im-PAES membranes, the Im-PAES-0.5 membrane was originally expected to have good performance in the VRB cell in consideration of its excellent resistance property to vanadium ions. However, the VRB cell assembled with Im-PAES-0.5 membrane can't even conduct charge–discharge cycling process at any current density above 80 mA cm^{-2}. This might be caused by the

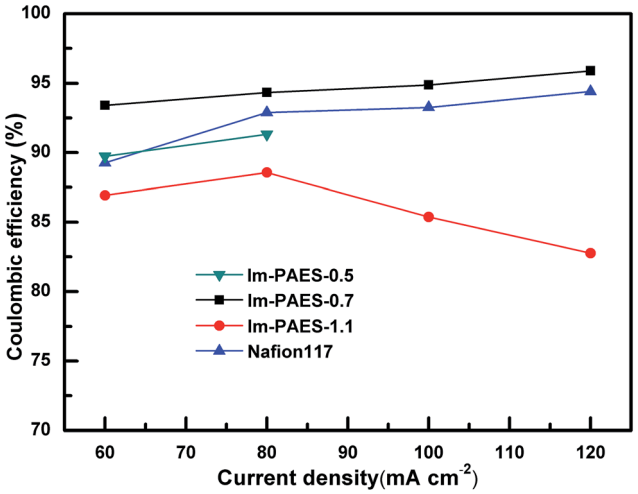

Fig. 6 Coulombic efficiencies of VRBs with Nafion 117 and Im-PAES membranes under different current densities.

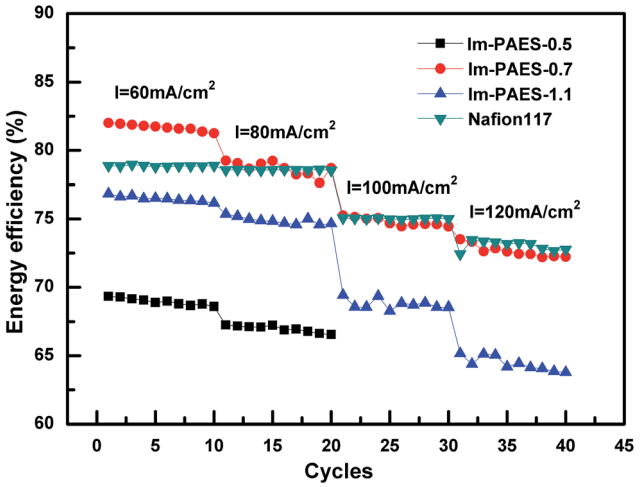

Fig. 8 Energy efficiencies and cycling durability of VRB cells with Nafion 117 and Im-PAES membranes at different current densities.

over-high ohmic polarization from intrinsic low IEC property of Im-PAES-0.5 membrane.

Fig. 7 illustrated the voltage efficiencies (VEs) of VRB cells assembled with Nafion 117 and Im-PAES membranes at different current densities. With the increase of charge–discharge current densities, the VEs of VRB cells with all the membranes exhibited significant decreasing trend, which was caused by the increase of ohmic resistance. Meanwhile, it can be found that the VE value of the VRB cells with Im-PAES-1.1 (from 88.0% to 77.5%) and Nafion 117 membrane (from 88.4% to 77.4%) exhibited almost identical decreasing trend, this might be attributed to their similar area resistances. The VRB cell with Im-PAES-0.7 membrane showed slightly lower VE value than that of VRB cell with Im-PAES-1.1 membrane from 60 to 120 mA cm^{-2}, 75.6% of voltage efficiency was obtained at high current density of 120 mA cm^{-2}.

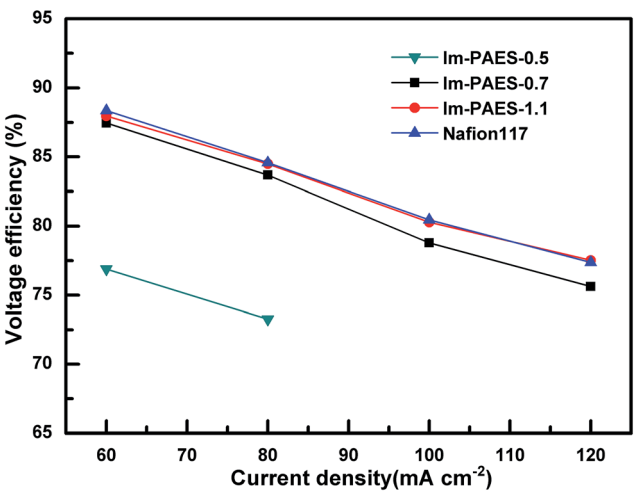

Fig. 7 Voltage efficiencies of VRB cells with Nafion 117 and Im-PAES membranes at different current densities.

Fig. 8 revealed the energy efficiencies (EEs) of VRB cells assembled with Im-PAES-0.5/0.7/1.1 and Nafion 117 membranes at the current densities of 60, 80, 100, 120 mA cm^{-2}. It was worth mentioning that average EE value was calculated and recognized as final EE result for every current density. Initially, at a current density of 60 mA cm^{-2}, the EE of cell with Im-PAES-0.7 membrane was slightly higher than that of cell with Nafion 117 (81.7% *vs.* 78.9%) within first 10 cycles. Furthermore, from 80 to 120 mA cm^{-2}, the EEs of cell with Im-PAES-0.7 (79.0%, 74.8%, 72.5%) showed the almost same level with that of VRB cell assembled with Nafion 117 (78.6%, 75.0%, 73.1%). This result supported that the cell with Im-PAES-0.7 membrane possessed as least comparable power density with that of cell with Nafion 117 under different current densities. In contrast, due to the high vanadium permeability and poor chemical stability of Im-PAES-1.1 membrane, lower EE values was obtained, *e.g.* only 76.5% at the current density of 60 mA cm^{-2}, decreasing dramatically with the increase of current density.

According to Fig. 8, stable performance and acceptable energy efficiency were still achieved in the cell with Im-PAES-0.7 membrane during the last 10 cycles at high current density of 120 mA cm^{-2}. This result further indicated that the Im-PAES-0.7 membrane could be comparable to Nafion 117 membrane for applications in VRB cell.

4. Conclusion

In summary, a serials of imidazolium functionalized poly(arylene ether sulfone) (Im-PAES) based anion exchange membranes for application in VRB were prepared in this work. The Im-PAES-0.5/0.7 membranes exhibited much lower vanadium ions permeability compared with Nafion 117 membrane. Meanwhile, among three anion exchange membranes, the highest ionic conductivity (up to 73.1 mS cm^{-1}) and excellent coulombic efficiency (up to 96.1%) could be achieved when the VRB cell assembled with the Im-PAES-0.7 membrane. The

chemical stability test in the strong oxidative VO_2^+ solution and the charge–discharge cycle performance tests at different current densities demonstrated that the Im-PAES-0.7 membrane possess comparable short-term stability to Nafion membranes. Considering all the properties mentioned above, the Im-PAES serials membranes could be potential alternatives for further VRB application.

Acknowledgements

The authors appreciate financial supports from Zhejiang Provincial Natural Science Foundation of China (No. LY15B020003), the Ministry of Science and Technology of China (No. 2014BAJ02B02), Zhejiang Province Preferential Post-doctoral Funded Project (No. BSH1402075) and Ningbo Natural Science Foundation (No. 2015A610243).

References

1 E. Sum, M. Rychcik and M. Skyllas-Kazacos, *J. Power Sources*, 1985, **16**, 85.
2 F. Rahmana and M. Skyllas-Kazacos, *J. Power Sources*, 2009, **189**, 1212.
3 M. H. Chakrabarti, R. W. Dryfe and E. P. L. Roberts, *Electrochim. Acta*, 2007, **52**, 2189.
4 M. Skyllas-Kazacos, M. H. Chakrabarti, S. A. Hajimolana, F. S. Mjalli and M. Saleem, *J. Electrochem. Soc.*, 2011, **158**, R55.
5 Z. S. Mai, H. M. Zhang, H. Z. Zhang, W. X. Xu, W. P. Wei, H. Na and X. F. Li, *ChemSusChem*, 2013, **6**, 328.
6 L. Joerissen, J. Garche, C. Fabjan and G. Tomazic, *J. Power Sources*, 2004, **127**, 98.
7 T. Mohammadi and M. Skyllas-Kazacos, *J. Membr. Sci.*, 1995, **98**, 77.
8 B. Schwenzer, J. L. Zhang, S. W. Kim, L. Y. Li, J. Liu and Z. G. Yang, *ChemSusChem.*, 2011, **4**, 1388.
9 H. Vafiadis and M. Skyllas-Kazacos, *J. Membr. Sci.*, 2006, **279**, 394.
10 T. Sukkar and M. Skyllas-Kazacos, *J. Appl. Electrochem.*, 2004, **34**, 137.
11 C. Jia, J. Liu and C. Yan, *J. Power Sources*, 2012, **203**, 190.
12 J. Xi, Z. Wu, X. Qu and L. Chen, *J. Power Sources*, 2007, **166**, 531.
13 Q. Luo, H. Zhang, J. Chen, P. Qian and Y. Zhai, *J. Membr. Sci.*, 2008, **311**, 98.
14 J. Y. Qiu, M. L. Zhai, J. H. Chen, Y. Wang, J. Peng, L. Xu, J. Q. Li and G. S. Wei, *J. Membr. Sci.*, 2009, **342**, 215.
15 D. Y. Chen, S. J. Wang, M. Xiao and Y. Z. Meng, *J. Power Sources*, 2010, **195**, 2089.
16 J. Y. Qiu, M. Y. Li, J. F. Ni, M. L. Zhai, J. Peng, L. Xu, H. H. Zhou, J. Q. Li and G. S. Wei, *J. Membr. Sci.*, 2007, **297**, 174.
17 Y. Wang, J. Y. Qiu, J. Peng, L. Xu, J. Q. Li and M. L. Zhai, *J. Membr. Sci.*, 2011, **376**, 70.
18 S. H. Zhang, C. X. Yin, D. B. Xing, D. L. Yang and X. G. Jian, *J. Membr. Sci.*, 2010, **363**, 243.
19 S. H. Zhang, B. G. Zhang, G. F. Zhao and X. G. Jian, *J. Mater. Chem. A*, 2014, **2**, 3083.
20 D. Y. Chen, M. A. Hickner, E. Agar and E. C. Kumbur, *Electrochem. Commun.*, 2013, **26**, 37.
21 T. Sata, S. Nojima and K. Matsusaki, *Polymer*, 1999, **40**, 7243.
22 Y. Li, T. W. Xu and M. Gong, *J. Membr. Sci.*, 2006, **279**, 200.
23 Y. Li and T. W. Xu, *J. Appl. Polym. Sci.*, 2009, **114**, 3016.
24 L. Franck-Lacaze, P. Sistat and P. Huguet, *J. Membr. Sci.*, 2009, **326**, 650.
25 M. S. Kang, Y. J. Choi and S. H. Moon, *AIChE J.*, 2003, **49**, 3213.
26 S. H. Zhang, B. G. Zhang, D. B. Xing and X. G. Jian, *J. Mater. Chem. A*, 2013, **1**, 12246.
27 D. Y. Chen, M. A. Hickner, E. Agar and E. C. Kumbur, *ACS Appl. Mater. Interfaces*, 2013, **5**, 7559.
28 S. Gu, R. Cai, T. Luo, Z. Chen, M. Sun, Y. Liu, G. He and Y. Yan, *Angew. Chem., Int. Ed.*, 2009, **48**, 6499.
29 H. Z. Zhang, H. M. Zhang, F. X. Zhang, X. F. Li, Y. Li and I. Vankelecom, *Energy Environ. Sci.*, 2013, **6**, 776.
30 L. C. Jheng, S. L. Hsu, B. Y. Lin and Y. L. Hsu, *J. Membr. Sci.*, 2014, **460**, 160.
31 X. C. Lin, X. H. Liang, S. D. Poynton, J. R. Varcoe, A. L. Ong, J. Ran, Y. Lin, Q. H. Li and T. W. Xu, *J. Membr. Sci.*, 2013, **443**, 193.
32 W. P. Wang, S. B. Wang, X. F. Xie, Y. F. Lv and V. K. Ramani, *J. Membr. Sci.*, 2014, **462**, 112.
33 S. C. Price, K. S. Williams and F. L. Beyer, *ACS Macro Lett.*, 2014, **3**, 160.
34 A. G. Wright and S. Holdcroft, *ACS Macro Lett.*, 2014, **3**, 444.
35 F. L. Gu, H. L. Dong, Y. Y. Li, Z. H. Si and F. Yan, *Macromolecules*, 2014, **47**, 208.
36 Z. H. Si, L. H. Qiu, H. L. Dong, F. L. Gu, Y. Y. Li and F. Yan, *ACS Appl. Mater. Interfaces*, 2014, **6**, 4346.
37 Y. Q. Yang, J. Wang, J. F. Zheng, S. H. Li and S. B. Zhang, *J. Membr. Sci.*, 2014, **467**, 48.
38 D. Y. Chen and M. A. Hickner, *ACS Appl. Mater. Interfaces*, 2012, **4**, 5775.
39 J. Fang, H. K. Xu, X. L. Wei, M. L. Guo, X. H. Lu, C. L. Lan, Y. M. Zhang, Y. Liu and T. Peng, *Polym. Adv. Technol.*, 2013, **24**, 168.
40 H. Y. Pan, S. X. Chen, Y. Y. Zhang, M. Jin, Z. H. Chang and H. T. Pu, *J. Membr. Sci.*, 2015, **476**, 87.
41 A. N. Lai, L. S. Wang, C. X. Lin, Y. Z. Zhuo, Q. G. Zhang and A. M. Zhu, *J. Membr. Sci.*, 2015, **481**, 9.